

## Fourier Analysis of Parallel Inexact Block-Jacobi Splitting with Transport Synthetic Acceleration in Slab Geometry

Massimiliano Rosa<sup>\*1</sup>, James S. Warsa<sup>2</sup> and Jae H. Chang<sup>2</sup>

<sup>1</sup>The Pennsylvania State University, 138 Reber Building, University Park,  
Pennsylvania PA 16802, U.S.A.

<sup>2</sup>Los Alamos National Laboratory, P.O. Box 1663, MS D409, Los Alamos,  
New Mexico NM 87545, U.S.A.

### Abstract

A Fourier analysis is conducted for the discrete-ordinates ( $S_N$ ) approximation of the neutron transport problem solved with Richardson iteration (Source Iteration) and Richardson iteration preconditioned with Transport Synthetic Acceleration (TSA), using the Parallel Block-Jacobi (PBJ) algorithm. Both “traditional” TSA (TTSA) and a “modified” TSA (MTSA), in which only the scattering in the low order equations is reduced by some non-negative factor  $\beta < 1$ , are considered.

The results for the un-accelerated algorithm show that convergence of the PBJ algorithm can degrade. The PBJ algorithm with TTSA can be effective provided the  $\beta$  parameter is properly tuned for a given scattering ratio  $c$ , but is potentially unstable. Compared to TTSA, MTSA is less sensitive to the choice of  $\beta$ , more effective for the same computational effort ( $c'$ ), and it is unconditionally stable.

**KEYWORDS:** *neutral particle transport, iterative acceleration, Fourier analysis, Transport Synthetic Acceleration, Parallel Block-Jacobi.*

## 1. Introduction

Fourier analysis is traditionally used to study transport iteration schemes in a homogeneous infinite medium. In fact, it represents a valuable tool to understand the behavior of the iteration error modes of various acceleration techniques, either in their continuous or spatially discretized forms.

In this paper we conduct a Fourier analysis for the discrete-ordinates ( $S_N$ ) approximation of the steady-state one-group transport problem solved with Richardson iteration (Source Iteration) and preconditioned Richardson iteration, using the Parallel Block-Jacobi (PBJ) algorithm. Two types of Transport Synthetic Acceleration (TSA) are utilized as preconditioners, the traditional “Beta” TSA [1] and a “modified” TSA. In the latter, the scattering in the low order equations is simply reduced by some non-negative factor less than unity. The spatial discretization employed is the Linear Discontinuous Finite Element Method (LDFEM) in slab geometry and the scattering is assumed to be isotropic.

The results of the infinite medium Fourier analysis agree with the numerical results of the PBJ algorithm for a finite-width slab as the number of parallel processors is increased. The numerical results also confirm that modified TSA (MTSA) can be used to efficiently precondition the PBJ algorithm for optically thin problems.

---

\* Corresponding author, Tel. 01-814-865-8429, E-mail: [mzr127@psu.edu](mailto:mzr127@psu.edu)

## 2. Fourier Analysis of Parallel Block-Jacobi (PBJ) Algorithm

### 2.1 Parallel Inexact Block-Jacobi Splitting

The homogeneous transport equation can be written, for isotropic scattering, in the following compact operator notation:

$$L\psi = S\phi \tag{1}$$

where  $L$  represents the “streaming plus total interaction” operator,  $S$  is the scattering operator,  $\psi$  is the angular flux, and  $\phi$  is the scalar flux. Furthermore, the scalar flux is the integral of the angular flux over all angles:

$$\phi = D\psi \tag{2}$$

where  $D$  is the “discrete-to-moment” operator.

In the PBJ algorithm, the incoming angular fluxes at the interface between two neighboring processors are “lagged” from the previous iteration. Therefore, we split the “streaming plus total interaction operator” into  $L_o$  (interior) and  $L_b$  (interface):

$$L = L_o + L_b. \tag{3}$$

The PBJ algorithm is then implemented through the following iteration scheme:

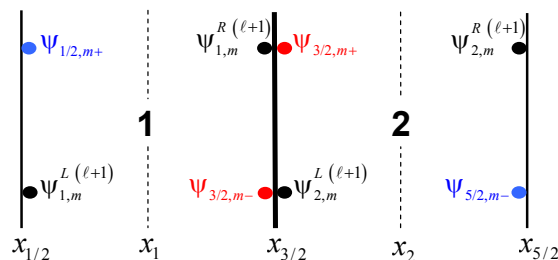
$$\psi^{(\ell+1)} = L_o^{-1} (SD - L_b) \psi^{(\ell)} \tag{4}$$

where  $\ell \geq 0$  is the iteration index. In this way, a formulation of the problem in terms of angular fluxes only is obtained. This formulation is convenient in order to devise a Fourier analysis for the PBJ algorithm, but is not actually utilized in its practical implementation. From a practical stand-point, a formulation of the algorithm in terms of scalar fluxes and interface angular fluxes is actually implemented to minimize storage requirements.

### 2.2 Fourier Analysis

The equations representing the fixed-source-free one-dimensional LDFEM [2] spatial discretization of the  $S_N$  approximation to Eq. (1) are written for the two-cell system of Fig. 1, in which the two computational cells share the interface between two adjacent processors.

**Figure 1:** Two-cell system for the Fourier analysis of PBJ.



The equations for the projections of the discrete-ordinates angular fluxes onto the linear basis functions of the finite element method, in the two neighboring cells, are grouped together for the discrete-ordinates characterized by positive and negative cosines respectively.

Different iteration indices have been used, in Fig. 1, to distinguish the unknowns that are being calculated in the current iteration from the angular fluxes available at the cells' interface and boundaries. The unknowns are the coefficients for the LDFEM basis functions' representation of the discrete-ordinates angular fluxes in the two cells,  $\psi_{i,m}^{L,R(\ell+1)}$  with cell index  $i=1,2$ . The angular fluxes  $\psi_{3/2,m-}$  ( $\psi_{3/2,m+}$ ) entering cell 1 (2) at the interface between the two cells, for the discrete-ordinates with negative (positive) cosine  $\mu_m$ , are known, in the PBJ algorithm, in terms of the angular fluxes  $\psi_{2,m}^{L(\ell)}$  ( $\psi_{1,m}^{R(\ell)}$ ) exiting from cell 2 (1), that have been determined in the previous iteration. This fact is accounted for through the following conditions.

#### Interface Conditions

$$\psi_{3/2,m+} = \psi_{1,m}^{R(\ell)} \quad (\mu_m > 0, \quad m = 1, \dots, N/2) \quad (5)$$

$$\psi_{3/2,m-} = \psi_{2,m}^{L(\ell)} \quad (\mu_m < 0, \quad m = N/2 + 1, \dots, N) \quad (6)$$

The angular fluxes  $\psi_{1/2,m+}$  ( $\psi_{5/2,m-}$ ) entering cell 1 (2) at the left (right) boundary of the two-cell system, for the discrete-ordinates with positive (negative) cosine  $\mu_m$ , are equal, as usual in a transport sweep of the spatial mesh, to the angular fluxes exiting from the upstream cell that has been previously swept in the current iteration. Since an infinite homogeneous medium, in which the two-cell system is periodically repeated, is considered in the Fourier analysis, the following ansatz is introduced.

#### Fourier Ansatz

$$\psi_{1/2,m+} = \psi_{2,m}^{R(\ell+1)} \exp(-j\lambda\sigma h), \quad m = 1, \dots, N/2 \quad (7)$$

$$\psi_{5/2,m-} = \psi_{1,m}^{L(\ell+1)} \exp(j\lambda\sigma h), \quad m = N/2 + 1, \dots, N \quad (8)$$

where  $j = \sqrt{-1}$  represents the imaginary unit,  $\sigma$  is the macroscopic total cross section for the homogeneous slab, while  $h = 2dx$  is the width of the two-cell system since  $x_{3/2} - x_{1/2} = x_{5/2} - x_{3/2} = dx$ . Finally,  $\lambda$  is the wave-number of the Fourier modes. As usual, the ansatz for the remaining unknown angular fluxes is:

$$\psi_{i,m}^{L,R(\ell)} = \omega^\ell d_{i,m}^{L,R} \exp(j\lambda\sigma x_{i\mp 1/2}), \quad i = 1, 2 \quad m = 1, \dots, N. \quad (9)$$

Substitution of Eqs. (5), (6), (7), (8) and (9) in the original LDFEM equations [2] leads, after considerable algebra, to the following Fourier domain matrix formulation for the PBJ algorithm:

$$\omega \mathbf{d} = \mathbf{F}^{-1}(\mathbf{BD} - \mathbf{C})\mathbf{d}. \quad (10)$$

In Eq. (10),  $\mathbf{d}$  is a vector containing the  $4N$  mode amplitudes  $d_{i,m}^{L,R}$ . Matrices  $\mathbf{F}$ ,  $\mathbf{C}$ ,  $\mathbf{B}$  and  $\mathbf{D}$  are the Fourier domain correspondents of the LDFEM spatial discretization for the  $S_N$  approximation to the  $L_o$ ,  $L_b$ ,  $S$  and  $D$  operators introduced in Eq. (4), respectively. These matrices have the following dependencies:

$$\mathbf{F} = \mathbf{F}(\text{dx}, \sigma, \boldsymbol{\mu}, \theta) \quad (11)$$

$$\mathbf{C} = \mathbf{C}(\boldsymbol{\mu}, \theta) \quad (12)$$

$$\mathbf{B} = \mathbf{B}(\text{dx}, c\sigma, \theta) \quad (13)$$

$$\mathbf{D} = \mathbf{D}(\mathbf{w}). \quad (14)$$

In Eqs. (11), (12), (13) and (14),  $c = \sigma_s / \sigma$  is the scattering ratio of the homogeneous slab while  $\boldsymbol{\mu}$  and  $\mathbf{w}$  are vectors containing the angle cosines and weights of the  $S_N$  quadrature, respectively. The short-hand parameter  $\theta = \lambda \sigma \text{dx}$  is used to express the argument of the complex exponential dependency of the matrices from the wave-number of the Fourier modes and the width of a cell, in mean-free-paths, deriving from the Fourier ansatz.

Notice the strict formal analogy between Eqs. (10) and (4), with matrices  $\mathbf{F}$  and  $\mathbf{C}$  corresponding to the interior and interface operators,  $L_o$  and  $L_b$ , respectively. The grouping of matrix  $\mathbf{C}$  with the other terms on the right hand side of Eq. (10) is representative of the “lagging” of the incoming angular fluxes, at the interface between two neighboring processors, from the previous iteration. Denoting as  $\mathbf{A}$  the matrix corresponding to the non-split  $L$  operator, the following expression corresponds, in the Fourier domain, to the operator splitting in Eq. (3):

$$\mathbf{A} = \mathbf{F}(\text{dx}, \sigma, \boldsymbol{\mu}, \theta) + \mathbf{C}(\boldsymbol{\mu}, \theta). \quad (15)$$

Rearranging Eq. (10), the following eigenvalue problem is finally obtained:

$$\omega \mathbf{d} = \mathbf{T}_{PBJ} \mathbf{d} \quad (16)$$

where:

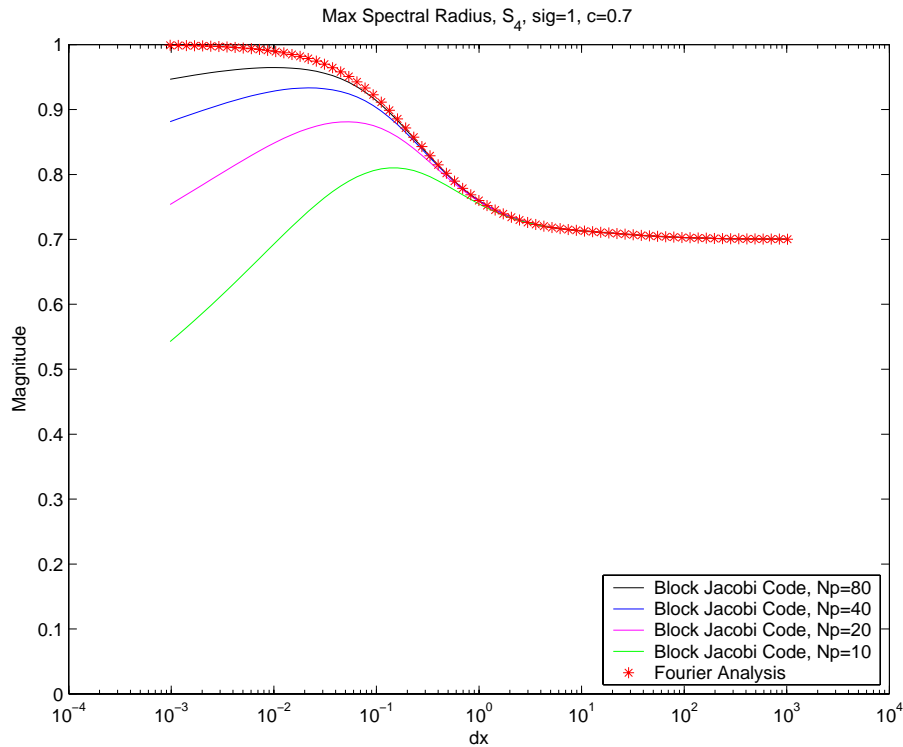
$$\mathbf{T}_{PBJ} = \mathbf{F}^{-1}(\mathbf{BD} - \mathbf{C}). \quad (17)$$

Equation (16) represents an eigenvalue problem for the iteration matrix  $\mathbf{T}_{PBJ}$  of the PBJ algorithm, with iteration eigenvalue  $\omega$  identified by the scalar introduced in Eq. (9). The eigenvalue with largest magnitude with respect to the Fourier parameter  $\theta$  is the spectral radius for the iterative algorithm. A spectral radius less than one implies convergence of the algorithm. Also, as the spectral radius decreases, the convergence rate increases.

In Fig. 2, we plot the spectral radius obtained, as a function of cell width, from the numerical implementation of the PBJ algorithm. The curves, determined by varying the

number of processors  $N_p$ , are compared with the value for the spectral radius predicted from the Fourier analysis. Two cells per processor are considered ( $N_c = 2$ ) and the scattering ratio is  $c = 0.7$ . Also the total cross section is  $\sigma = 1$  and the quadrature is the Gauss  $S_4$  quadrature.

**Figure 2:** Fourier analysis and finite-slab spectral radius of PBJ ( $N_c = 2$ ).



The results shown in Fig. 2 can be understood in view of the fact that, while the theoretical spectrum from the Fourier analysis is obtained for an infinite medium, the actual spectrum incorporates the effect of particle leakage at the boundaries of the finite-width slab.

As the cell width is increased, and the slab becomes optically thick, the effect of leakage is less and less important. Therefore the curves obtained varying  $N_p$  are coincident with one another, and with the theoretically predicted trend, in the optically thick slab regime. As the cell width is decreased, the effect of leakage becomes dominant and the curves depart from the infinite medium trend. As expected, though, the actual spectral radius approaches the theoretical value as the number of processors is increased, making the overall slab thicker. The theoretical curve would ideally be obtained in the limit as  $N_p \rightarrow \infty$ .

Overall, the results obtained point to the fact that convergence of the PBJ algorithm can degrade for optically thin problems, even for values of the scattering ratio  $c$  less than unity. In fact, the limit value of one obtained for the spectral radius, as the cell width is decreased, is independent from the value of  $c$ .

### 3. Fourier analysis of PBJ with Transport Synthetic Acceleration (TSA)

#### 3.1 Introduction

The results obtained in the previous section indicate that preconditioning of the PBJ

algorithm is necessary in order to improve its spectral properties, especially for optically thin problems. In this section, we use Transport Synthetic Acceleration (TSA) as a preconditioner. The complete explanation of TSA can be found in [1]. We incorporate both the traditional TSA (TTSA) introduced in [1] and a modified TSA (MTSA), where only the scattering in the low order equations is reduced by some non-negative factor  $\beta$  less than unity.

In both the resulting schemes for the acceleration of the PBJ algorithm, Eq. (4) is now the first step (high order equation) in a two-step process for the determination of the angular flux in the current iteration:

$$\Psi^{(\ell+1/2)} = L_o^{-1} (SD - L_b) \Psi^{(\ell)}. \quad (18)$$

The second step (low order equation) consists of the determination of an additive correction  $f^{(\ell+1/2)}$  satisfying the equation:

$$Pf^{(\ell+1/2)} = (SD - L_b) (\Psi^{(\ell+1/2)} - \Psi^{(\ell)}) \quad (19)$$

where  $P$  is a low order approximation to the full transport operator  $(L - SD)$ . This approximation amounts to solving a transport problem in which the  $L$  operator is not split. The transport problem is anyway solved at a lower computational cost, since the effective scattering ratio  $c'$  [1] is lowered by the introduction of a suitable non-negative parameter  $\beta \in [0,1]$ . Also, in the PBJ algorithm accelerated with TSA, interface residual terms from the high order equation are introduced in the low order equation and are “lagged” from the previous step in the current iteration by means of the  $L_b$  interface operator. Therefore, these residual terms act as a sort of additional negative sources (sinks) of neutrons at the interface between two neighboring processors in the low order equation. Finally, the update equation for the angular flux becomes:

$$\Psi^{(\ell+1)} = \Psi^{(\ell+1/2)} + f^{(\ell+1/2)}. \quad (20)$$

### 3.2 Fourier Analysis for PBJ with TTSA

The Fourier analysis outlined in Section 2.2 is extended to the PBJ algorithm with TTSA. The formulation for the high order equations is the same as in the Fourier analysis previously developed for PBJ. In addition to the interface conditions and Fourier ansatz for the high order problem, a similar set of equations is developed for the low order problem.

#### Interface Conditions plus Residual Terms from High Order Equations

$$f_{3/2,m+} = f_{1,m}^{R(\ell+1/2)} + \left( \Psi_{1,m}^{R(\ell+1/2)} - \Psi_{1,m}^{R(\ell)} \right), \quad m = 1, \dots, N/2 \quad (21)$$

$$f_{3/2,m-} = f_{2,m}^{L(\ell+1/2)} + \left( \Psi_{2,m}^{L(\ell+1/2)} - \Psi_{2,m}^{L(\ell)} \right), \quad m = N/2 + 1, \dots, N \quad (22)$$

#### Fourier Ansatz

$$f_{1/2,m+} = f_{2,m}^{R(\ell+1)} \exp(-j\lambda\sigma h), \quad m = 1, \dots, N/2 \quad (23)$$

$$f_{5/2,m-} = f_{1,m}^{L(\ell+1)} \exp(j\lambda\sigma h), \quad m = N/2 + 1, \dots, N \quad (24)$$

As usual, the ansatz for the remaining unknown angular fluxes and additive corrections is:

$$\psi_{i,m}^{L,R(\ell+1/2)} = \omega^\ell e_{i,m}^{L,R} \exp(j\lambda\sigma x_{i\mp 1/2}), \quad i = 1, 2 \quad m = 1, \dots, N \quad (25)$$

$$f_{i,m}^{L,R(\ell+1/2)} = \omega^\ell f_{i,m}^{L,R} \exp(j\lambda\sigma x_{i\mp 1/2}), \quad i = 1, 2 \quad m = 1, \dots, N. \quad (26)$$

When the augmented interface conditions and Fourier ansatz are substituted in the LDFEM equations for PBJ with TTSA, the following Fourier domain matrix formulation is obtained:

$$\mathbf{e} = \mathbf{F}^{-1} (\mathbf{BD} - \mathbf{C}) \mathbf{d} \quad (27)$$

$$\bar{\mathbf{A}} \mathbf{f} = (1 - \beta) \mathbf{B} \mathbf{d} \mathbf{f} + (\mathbf{BD} - \mathbf{C})(\mathbf{e} - \mathbf{d}) \quad (28)$$

$$\omega \mathbf{d} = \mathbf{e} + \mathbf{f}. \quad (29)$$

In Eqs. (27), (28) and (29),  $\mathbf{e}$  and  $\mathbf{f}$  are vectors containing the  $4N$  mode amplitudes  $e_{i,m}^{L,R}$  and  $f_{i,m}^{L,R}$  respectively. Equation (27) represents the high order equation and has the same form as Eq. (10). Equation (28) is the low order equation for PBJ with TTSA. Consistently with [1], a reduced scattering cross section  $\sigma_{S,TTSA} = (1 - \beta)c\sigma$  is introduced in the scattering matrix  $\mathbf{B}$  multiplying the residual vector  $\mathbf{f}$  on the right hand side. The effect of this substitution is equivalent to multiplying the whole matrix  $\mathbf{B}$  by the factor  $(1 - \beta)$ . Matrix  $\bar{\mathbf{A}}$ , on the left hand side, is the same matrix, corresponding to the non-split “streaming plus total interaction” operator  $L$ , previously defined in Eq. (15) but evaluated for the reduced total cross section  $\sigma_{TTSA} = (1 - \beta)c$ :

$$\bar{\mathbf{A}} = \mathbf{F}(\mathbf{dx}, \sigma_{TTSA}, \boldsymbol{\mu}, \theta) + \mathbf{C}(\boldsymbol{\mu}, \theta). \quad (30)$$

As mentioned before, the full non-split transport problem is exactly solved in the low order equation, but at a reduced computational cost. In fact, the effective scattering ratio for this transport problem is [1]:

$$c'_{TTSA} = \frac{\sigma_{S,TTSA}}{\sigma_{TTSA}} = \frac{(1 - \beta)}{(1 - \beta c)} c < c, \quad \text{for } \beta > 0. \quad (31)$$

Note also the negative contribution of the residual terms from the high order equation, introduced in Eqs. (21) and (22), on the right hand side of Eq. (28). In particular, notice that these terms are “lagged” by means of the same matrix  $\mathbf{C}$  appearing in Eq. (27).

Finally, Eq. (29) represents the update equation in the Fourier domain. Eliminating vectors  $\mathbf{e}$  and  $\mathbf{f}$  from Eqs. (27), (28) and (29), the following eigenvalue problem is finally obtained:

$$\omega \mathbf{d} = \mathbf{T}_{TTSA} \mathbf{d} \quad (32)$$

where:

$$\mathbf{T}_{TTSA} = \mathbf{T}_{PBJ} + [\bar{\mathbf{A}} - (1-\beta)\mathbf{BD}]^{-1} (\mathbf{BD} - \mathbf{C})(\mathbf{T}_{PBJ} - \mathbf{I}). \quad (33)$$

Equation (32) represents an eigenvalue problem for the iteration matrix  $\mathbf{T}_{TTSA}$  of the PBJ algorithm with TTSA preconditioner. As usual,  $\mathbf{I}$  is the identity matrix. The eigenvalue with largest magnitude with respect to the Fourier parameter  $\theta$  is the spectral radius for the accelerated iterative algorithm.

### 3.3 Fourier Analysis for PBJ with MTSA

The Fourier domain matrix formulation for PBJ with MTSA is comprised of the same high order and update equations as for PBJ with TTSA, Eqs. (27) and (29). The low order equation for PBJ with TTSA, Eq. (28), is instead replaced by the following:

$$\mathbf{A}\mathbf{f} = \beta\mathbf{B}\mathbf{D}\mathbf{f} + (\mathbf{BD} - \mathbf{C})(\mathbf{e} - \mathbf{d}). \quad (34)$$

Matrix  $\mathbf{A}$  is now exactly the same as in Eq. (15). In MTSA, only matrix  $\mathbf{B}$ , multiplying the residual vector  $\mathbf{f}$  on the right hand side, is reduced by a factor  $\beta \in [0,1]$ , which leads to the scattering cross section  $\sigma_{s,MTSA} = \beta c \sigma$  in the low order equation. This leads to the following effective scattering ratio for the low order transport problem:

$$c'_{MTSA} = \frac{\sigma_{s,MTSA}}{\sigma} = \beta c < c, \quad \text{for } \beta < 1. \quad (35)$$

Eliminating vectors  $\mathbf{e}$  and  $\mathbf{f}$  from Eqs. (27), (29) and (34), the following eigenvalue problem is finally obtained:

$$\omega \mathbf{d} = \mathbf{T}_{MTSA} \mathbf{d} \quad (36)$$

where:

$$\mathbf{T}_{MTSA} = \mathbf{T}_{PBJ} + [\mathbf{A} - \beta\mathbf{BD}]^{-1} (\mathbf{BD} - \mathbf{C})(\mathbf{T}_{PBJ} - \mathbf{I}). \quad (37)$$

Equation (36) represents an eigenvalue problem for the iteration matrix  $\mathbf{T}_{MTSA}$  of the PBJ algorithm with MTSA preconditioner.

### 3.4 Comparison of PBJ with TTSA and PBJ with MTSA

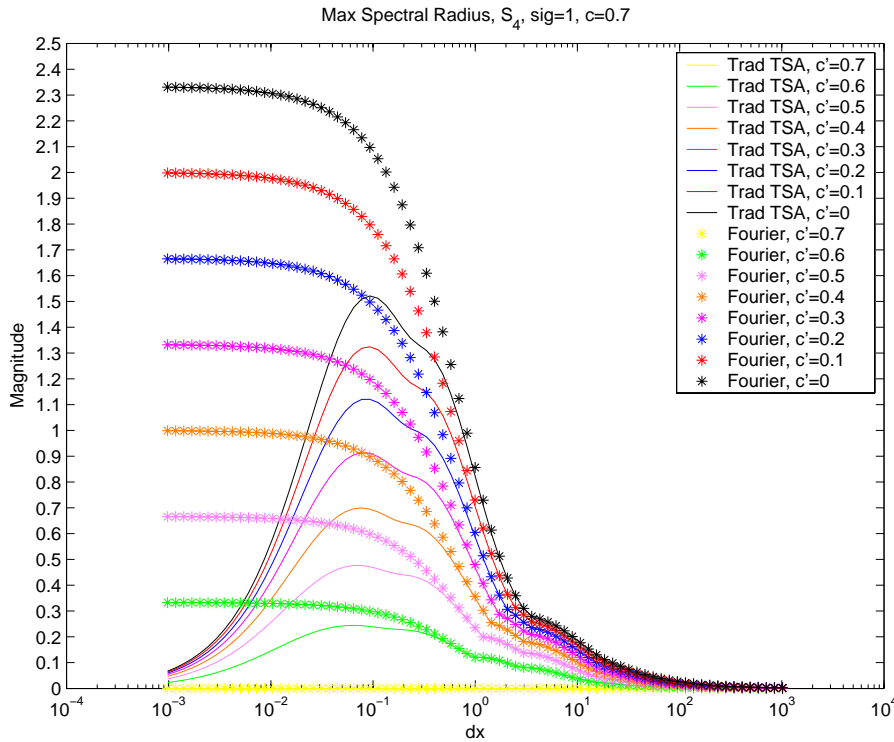
Since the effective scattering ratio  $c'$  is a measure of the actual computational effort required by each TSA acceleration method, a comparison of the two methods has to be considered for equal values of this parameter and not for the same value of  $\beta$ , that would result in different values for  $c'_{TTSA}$  and  $c'_{MTSA}$ , as is evident from Eqs. (31) and (35). In

particular, the closer the value of  $c$  is to unity, the slower the variation of  $c'_{TTSA}$  with respect to  $c'_{MTSA}$  for a given increment of  $\beta$ .

In Fig. 3, we plot the spectral radius obtained, as a function of cell width, from the numerical implementation of PBJ with TTSA, for a finite-width slab in the case of 40 parallel processors ( $N_p=40$ ) with two cells per processor ( $N_c=2$ ). The curves, determined varying the effective scattering ratio  $c'$ , are compared with the value for the spectral radius predicted from the infinite medium Fourier analysis. This figure has been obtained for the  $S_4$  quadrature considering a slab with unit total cross section and scattering ratio  $c = 0.7$ .

The comparison of the curves obtained from the numerical implementation of PBJ with MTSA with the value of the spectral radius predicted from the corresponding Fourier analysis is presented in Fig. 4.

**Figure 3:** Fourier analysis and finite-slab spectral radius of PBJ wt TTSA ( $N_p = 40, N_c = 2$ ).

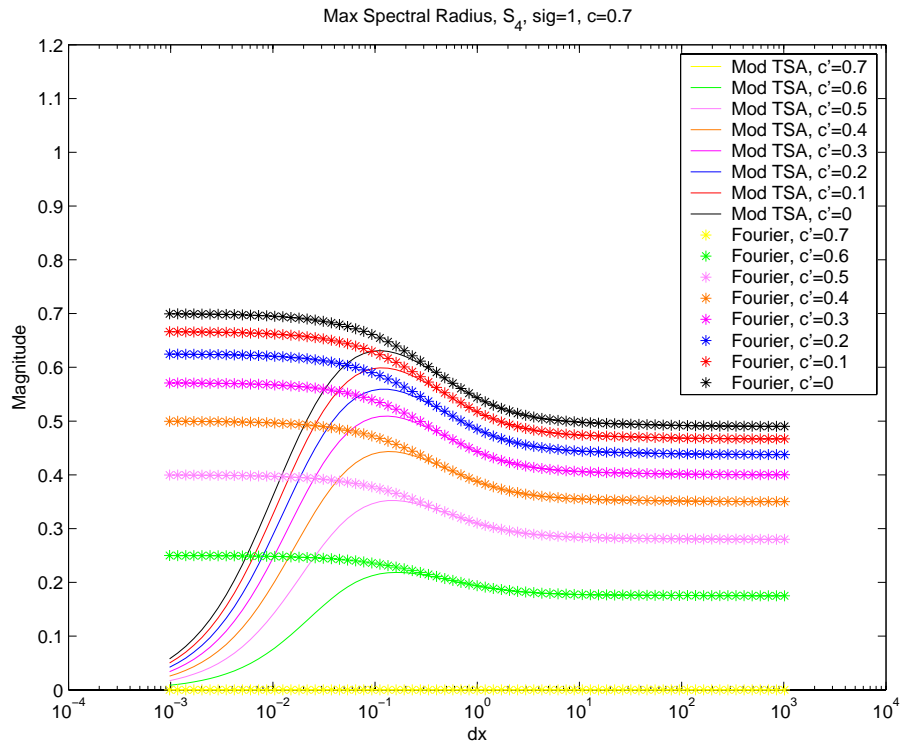


As predicted by the Fourier analysis, the PBJ algorithm accelerated with TTSA may potentially diverge for some thin problems if the  $\beta$  parameter is not conveniently tuned (Fig. 3). On the other hand, the PBJ algorithm accelerated with MTSA does not diverge for optically thin problems (Fig. 4). As a matter of fact, the spectral radius predicted from the Fourier analysis for PBJ with MTSA is bounded from above by the value of the scattering ratio  $c$  for any possible value of the  $\beta$  parameter. Compared to TTSA, not only MTSA appears to be less sensitive to the choice of  $\beta$ , but also more effective for the same computational effort ( $c'$ ) in the optically thin regime.

Notice that, both in Figs. 3 and 4, as  $dx$  decreases from  $10^{-1}$  the actual spectral radius for both TSA methods also decreases, departing from the value predicted by the Fourier analysis. This is due to particle leakage at the boundaries of the finite-width slab in the numerical problem. Finally, as far as the optically thick slab regime is concerned, the non-zero value for the MTSA spectral radius (Fig. 4), as opposed to the zero value exhibited by TTSA (Fig. 3), may in any case be made conveniently

small by a suitable tuning of the effective scattering ratio  $c'$  through the  $\beta$  parameter.

**Figure 4:** Fourier analysis and finite-slab spectral radius of PBJ wt MTSA ( $N_p = 40, N_c = 2$ ).



## 4. Conclusion

A Fourier analysis has been implemented for the Parallel Block-Jacobi (PBJ) algorithm and for PBJ with Transport Synthetic Acceleration (TSA) using both traditional TSA (TTSA) and a modified TSA (MTSA), in which the scattering in the low order equations is reduced by some non-negative factor  $\beta < 1$ . The results for the un-accelerated algorithm show that convergence of PBJ can degrade. The PBJ algorithm with TTSA can be effective provided the  $\beta$  parameter is properly tuned for a given scattering ratio  $c$ , but is potentially unstable. Compared to TTSA, MTSA is less sensitive to the choice of  $\beta$ , more effective for the same computational effort ( $c'$ ), and it is unconditionally stable.

## Acknowledgments

This work was performed under US Government Contract W-7405-ENG-36 for Los Alamos National Laboratory, which is operated by the University of California for the US Department of Energy.

## References

- 1) G. L. Ramone, M. L. Adams and P. F. Nowak, "A Transport Synthetic Acceleration Method for Transport Iterations," Nucl. Sci. Eng. **125**, 257-283 (1997).
- 2) R. E. Alcouffe, E. W. Larsen, W. F. Miller, Jr., and B. R. Wienke, "Computational Efficiency of Numerical Methods for the Multigroup, Discrete-Ordinates Neutron Transport Equations: The Slab Geometry Case," Nucl. Sci. Eng. **71**, 111-127 (1979).